

See discussions, stats, and author profiles for this publication at: <https://www.researchgate.net/publication/231653461>

# Layer-by-Layer Assembly of Carbon Nanotubes Incorporated in Light-Addressable Potentiometric Sensors

ARTICLE in THE JOURNAL OF PHYSICAL CHEMISTRY C · AUGUST 2009

Impact Factor: 4.77 · DOI: 10.1021/jp904777t

CITATIONS

41

READS

39

7 AUTHORS, INCLUDING:



[José Roberto Siqueira Jr.](#)

Universidade Federal do Triângulo Mineiro...

25 PUBLICATIONS 530 CITATIONS

SEE PROFILE



[Arshak Poghosian](#)

Fachhochschule Aachen

198 PUBLICATIONS 2,400 CITATIONS

SEE PROFILE



[Valtencir Zucolotto](#)

University of São Paulo

163 PUBLICATIONS 2,677 CITATIONS

SEE PROFILE



[Osvaldo N Oliveira](#)

University of São Paulo

531 PUBLICATIONS 8,971 CITATIONS

SEE PROFILE

# Layer-by-Layer Assembly of Carbon Nanotubes Incorporated in Light-Addressable Potentiometric Sensors

José R. Siqueira, Jr.,<sup>†,‡,§</sup> Carl F. Werner,<sup>‡,§</sup> Matthias Bäcker,<sup>‡,§</sup> Arshak Poghosian,<sup>‡,§</sup> Valtencir Zucolotto,<sup>†</sup> Osvaldo N. Oliveira, Jr.,<sup>\*,†</sup> and Michael J. Schöningh<sup>\*,‡,§</sup>

Physics Institute of São Carlos, University of São Paulo, 369 São Carlos, Brazil, Institute of Nano- and Biotechnologies, Aachen University of Applied Sciences, 52428 Jülich, Germany, and Institute of Bio- and Nanosystems (IBN2), Research Centre Jülich, 52425 Jülich, Germany

Received: May 21, 2009; Revised Manuscript Received: July 6, 2009

The integration of carbon nanotubes in conjunction with a chemical or biological recognition element into a semiconductor field-effect device (FED) may lead to new (bio)chemical sensors. In this study, we present a new concept to develop field-effect-based sensors, using a light-addressable potentiometric sensor (LAPS) platform modified with layer-by-layer (LbL) films of single-walled carbon nanotubes (SWNTs) and polyamidoamine (PAMAM) dendrimers. Film growth was monitored for each layer adsorbed on the LAPS chip by measuring current–voltage (*I/V*) curves. The morphology of the films was analyzed via atomic force microscopy (AFM) and field-emission scanning electron microscopy (FESEM), revealing the formation of a highly interconnected nanostructure of SWNTs-network into the dendrimer layers. Constant current (CC) measurements showed that the incorporation of the PAMAM/SWNT LbL film containing up to 6 bilayers onto the LAPS structure has a high pH sensitivity of ca. 58 mV/pH. The biosensing ability of the devices was tested for penicillin G via adsorptive immobilization of the enzyme penicillinase atop the LbL film. LAPS architectures modified with the LbL film exhibited higher sensitivity, ca. 100 mV/decade, in comparison to ca. 79 mV/decade for an unmodified LAPS, which demonstrates the potential application of the CNT-LbL structure in field-effect-based (bio)chemical sensors.

## 1. Introduction

Among the multitude of chemical sensors and biosensors, silicon-based (bio)chemical sensors are attractive owing to the possible combination of chemical and biological recognition processes with silicon chip manufacturing.<sup>1–3</sup> In field-effect devices (FEDs) derived from metal–insulator–semiconductor or insulated-gate field-effect transistors, in particular, the gate electrode is replaced by a sensitive layer, an electrolyte solution (test sample), and a reference electrode.<sup>1–3</sup> Any interaction at the electrolyte interface with an ion- and/or charge-sensitive gate layer affects the response from the FEDs.<sup>1–3</sup> Capacitive electrolyte–insulator–semiconductor (EIS) sensors, ion-sensitive field-effect transistors (ISFETs), and light-addressable potentiometric sensors (LAPS) represent typical examples of FEDs, which may form the basis of a new generation of (bio)chemical microsensors.<sup>1–3</sup> Such FED sensors are readily processable into miniaturized devices and may be used in various applications.<sup>1–5</sup>

LAPS are a particularly promising platform for multisensors and lab-on-chip devices, with the same structure as capacitive EIS sensors.<sup>1,3,6–9</sup> The area of the sensing surface, however, is defined by illumination by using a modulated light beam, which induces an ac photocurrent as the sensor signal.<sup>1,3,6–9</sup> LAPS devices have been applied in chemically and biologically related subjects such as the detection of bacteria growth and the measurement of cell metabolisms.<sup>1,3,6–9</sup> Other applications

include LAPS devices to measure pH, redox potential, and ion and analyte concentrations by modifying the sensing surface with adequate transducer materials.<sup>1,3,9</sup>

With regard to transducer materials, carbon nanotubes (CNTs) have been largely used in sensing and biosensing,<sup>10–16</sup> taking advantage of their electrical properties and high surface areas.<sup>10–13</sup> The assembly of CNTs for a sensing device may be in the form of an ultrathin film, which can be produced with the electrostatic layer-by-layer technique (LbL) that allows fine control over film thickness and architecture.<sup>17–22</sup> In addition, this method allows for CNTs to be assembled with various types of materials, including enzymes, nanoparticles, and polymers, in a way to provide synergy among the constituents of the film.<sup>23–26</sup>

In this study, we report for the first time on the LbL assembly of single-walled carbon nanotubes (SWNTs) incorporated on a LAPS structure (LAPS-NT). The nanostructured film was prepared by alternating layers of functionalized SWNTs with layers of the polyamidoamine (PAMAM) dendrimer. The influence from the film morphology changes induced by incorporation of the nanotubes on the sensor signal is discussed, and the feasibility of a LAPS-NT biosensor for penicillin detection is demonstrated.

## 2. Experimental Section

### 2.1. Fabrication and Characterization of LAPS Devices.

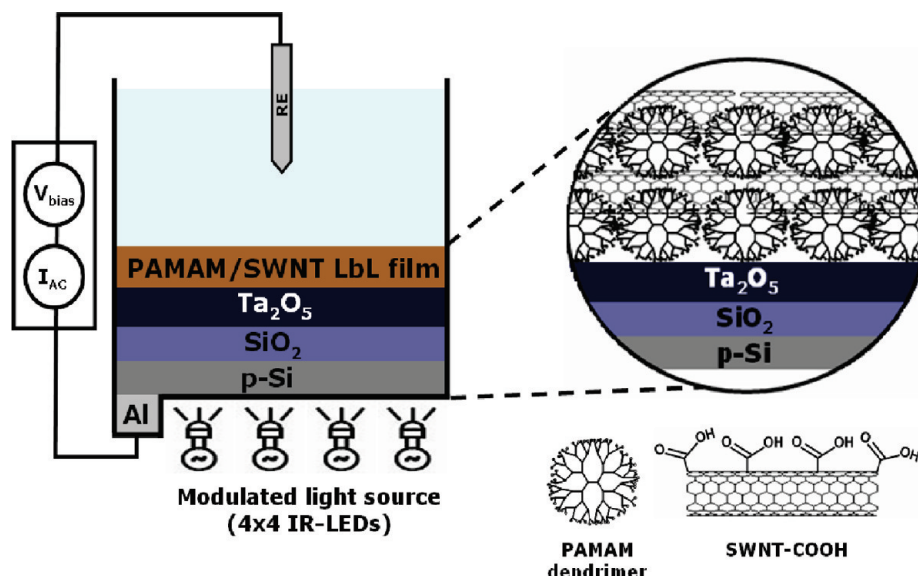
The electronic units of the LAPS devices were implemented with surface mounted devices (SMD) with 16 spots of infrared light-emitting diodes (IR-LEDs).<sup>8</sup> The LAPS structure of p-Si-SiO<sub>2</sub>-Ta<sub>2</sub>O<sub>5</sub> was prepared on a p-type Si(100) wafer (356–406 μm in thickness, 1–10 Ωcm) by forming a 30-nm-thick SiO<sub>2</sub>

\* To whom correspondence should be addressed. M.J.S.: e-mail m.j.schoening@fz-juelich.de, phone +49 (0) 241-6009-53215. O.N.O.: e-mail chu@ifsc.usp.br, phone +55 16 3373-9825.

<sup>†</sup> University of São Paulo.

<sup>‡</sup> Aachen University of Applied Sciences.

<sup>§</sup> Research Centre Jülich.

**SCHEME 1: Schematic Representation of the LAPS Structure Functionalized with a PAMAM/SWNT LbL Film, and Chemical Structure of the Materials Employed**


layer via thermal oxidation of Si in an O<sub>2</sub> atmosphere at 1050 °C for 30 min, while a 55-nm-thick Ta<sub>2</sub>O<sub>5</sub> layer was prepared via electron-beam evaporation of 30 nm Ta, followed by thermal oxidation at 515 °C during 30 min. A 300-nm-thick Al contact layer was deposited on the rear-side of the p-Si wafer, which was cut into 20 mm × 20 mm chips. The Al rear contact was partly removed for illumination. The sensor chip was mounted in a homemade measuring cell of Teflon and sealed with a silicone ring. An area of 2.25 cm<sup>2</sup> on the sensor surface was exposed to the test solution and illuminated by 16 IR-LEDs from the back side. Scheme 1 illustrates a representation of the LAPS setup and its operation principle.

The LAPS sensors were characterized by using current–voltage (*I/V*) and constant-current (CC) modes. For the *I/V* curve, the photocurrent signal was measured as a function of the external bias voltage, while the ion concentration was determined by measuring the horizontal shift of the *I/V* curve. After specifying the measurement parameters, such as the range of bias voltage and the number of measurements to be repeated, up to 16 *I/V* curves—corresponding to each measuring spot—were simultaneously obtained. The *I/V* measurements were used to define the working point for the CC-mode measurement. The optimal working point was found at the highest slope in the *I/V* curve. Therefore, after taking the 16 *I/V* curves, it was possible to calculate and set the working point for the subsequent CC-mode measurement. To record the temporal change of the ion concentration in the solution, the LAPS device was operated in the CC mode, where the bias voltage was controlled by a feedback loop to maintain a fixed photocurrent.<sup>7</sup>

**2.2. Materials and Solutions.** The carboxylic acid functionalized SWNTs and the G4 PAMAM dendrimer were acquired from Sigma-Aldrich. These nanotubes with mainly semiconductor features were produced with the arc discharge technique, having a nominal purity of 95%, length of 0.5–1.5 μm, and diameter of 1.5 and 3–5 nm for individual and bundled samples, respectively. Titrisol buffered solutions at pH 4 and 8 were used to prepare PAMAM and SWNTs solutions, respectively, at concentrations of 1.0 g L<sup>-1</sup>. An aqueous dispersion was obtained by adding 10 mg of SWNT into 10 mL of the buffer solution under ultrasonication for 2 h, which was then filtered. The enzyme penicillinase (*Bacillus cereus*, 1670 units/mg protein,

from Sigma) was prepared in 0.2 mol L<sup>-1</sup> triethanolamine (TEA) buffer at pH 8. The enzyme was immobilized by dropping 80 μL of solution on top of the sensor surface, and then dried at room temperature for 4 h. Penicillin G (benzyl penicillin, C<sub>16</sub>H<sub>17</sub>N<sub>2</sub>O<sub>4</sub>SN<sub>a</sub>, from Sigma) was prepared in 0.5 × 10<sup>-3</sup> mol L<sup>-1</sup> polymix buffer, pH 8, containing 0.1 mol L<sup>-1</sup> KCl solution at concentrations ranging from 0.5 × 10<sup>-3</sup> to 5.0 × 10<sup>-3</sup> mol L<sup>-1</sup>.

**2.3. Fabrication and Characterization of LbL Films.** LbL films were assembled by combining SWNTs with the polyamidoamine (PAMAM) dendrimer in a homemade measuring cell, sealed by silicone, via alternated dropping of PAMAM (5 min) and SWNT (10 min) solutions into the cell, followed by rinsing and drying steps (see the idealized LbL film structure in Scheme 1). The surface morphology of the LAPS containing the PAMAM/SWNT LbL film (LAPS-NT) was analyzed with an atomic force microscope (AFM) BioMat Workstation (JPK Instruments, Germany) and a field-emission scanning electron microscope (FESEM) Gemini Column LEO 1550 VP (Germany). The LAPS-NT sensors with a contact area of 2.25 cm<sup>2</sup> were characterized by using *I/V* and CC methods at a frequency of 1 kHz in a bias voltage range from -0.8 to 1.2 V, with a step width of 20 mV and an Ag/AgCl reference (Metrohm) electrode.

### 3. Results and Discussion

**3.1. Monitoring the Adsorption of LbL Multilayers by Using a LAPS Platform.** FEDs are capable of detecting charged macromolecules, which may be useful for investigating molecular interactions at liquid/solid interfaces that are involved in many systems akin to materials science and nanotechnology.<sup>2,27,28</sup> Indeed, FEDs were used to monitor the growth of LbL multilayers with the advantage of identifying contributions from each adsorbed layer to the sensor signal.<sup>2,27,28</sup> In particular, LAPS can offer the possibility of monitoring the multilayer formation in different places on the chip, since *I/V* curves are obtained for distinct spots illuminated with 16 IR-LEDs. Figure 1 shows *I/V* curves of one spot measured in a buffer solution at pH 7 for a LAPS-NT containing from 1 to 9 bilayers (Figure 1a). The zoom of the depletion range at a working point of ca. 1.0 μA and the corresponding potentials for each PAMAM and



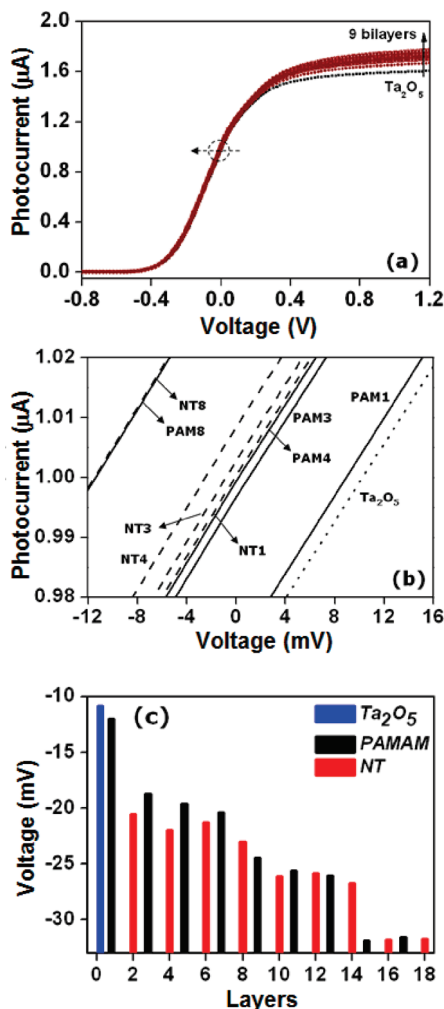


**Figure 1.** *I/V* curves for a LAPS chip functionalized with multilayers of PAMAM/SWNT measured in a buffer solution at pH 7 (a), detailed zoom in the depletion range at a working point of 1.0  $\mu$ A (b), and potential shifts evaluated from the *I/V* curves as a function of the adsorbed PAMAM or SWNT layer number (c).

SWNTs adsorbed layers are shown in Figure 1, panels b and c, respectively. It is important to note the similarity of the 16 *I/V* curves, which is evidence of a homogeneous film formation over the entire chip surface.

The alternated adsorption of charged layers of PAMAM ( $\text{NH}_3^+$ ) and SWNTs ( $\text{COO}^-$ ) caused a shift in the *I/V* curves along the bias voltage axis, as depicted in Figure 1b. This may be explained with the same concept used in detecting charged macromolecules in capacitive EIS sensors,<sup>2,27,28</sup> as the field-effect structure employed (p-Si-SiO<sub>2</sub>-Ta<sub>2</sub>O<sub>5</sub>) was identical. The potential shifts in the *I/V* curves arise from the charge of the adsorbed outermost layer of the film. An excess of positive or negative noncompensated charges are expected for PAMAM or SWNTs, respectively. This is accompanied by a potential difference across the solid/liquid interface, and the direction of the shifts depends on the sign of the charge of the outermost layer. Therefore, the positively charged dendrimers and the negatively charged SWNTs induce an interfacial potential change resulting in a change in the flat-band voltage of the LAPS structure. Similar results were obtained with the same film architecture for a capacitive EIS structure.<sup>29</sup> The latter presented larger potential shifts and the adsorption of the layers tended to saturate after approximately 8 layers, analogously to that observed for the LAPS structure. The latter, however, presented

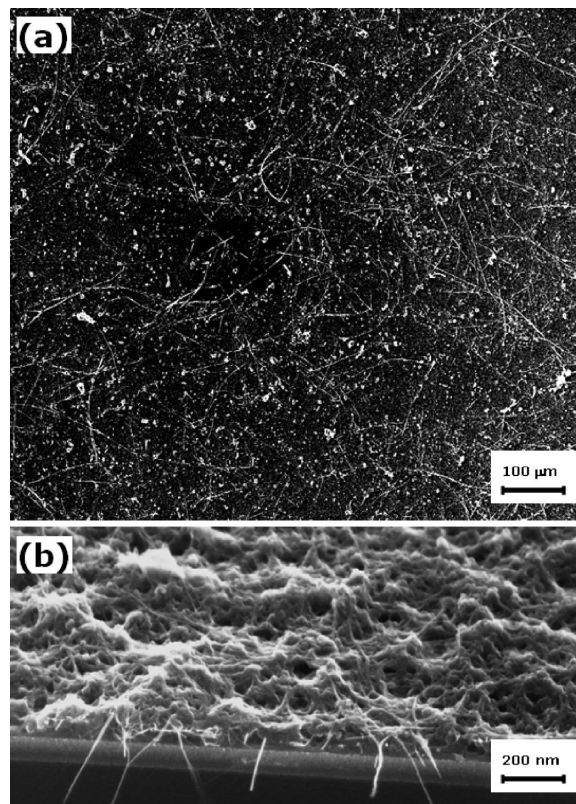


**Figure 2.** FESEM images for a 6-bilayer PAMAM/SWNT LbL film: top view (a) and cross-sectional view (b).

a new adsorption signal after 16 layers and pointed to saturation again, as shown in Figure 1c. This potential shift might be related to a redistribution of ions (including protons) within the porous film as the multilayers rearrange themselves on the film surface.<sup>27–29</sup>

**3.2. Surface Morphology of the LbL Films on LAPS Chips.** The sensing area of a LAPS chip is 3-fold larger than the EIS area,<sup>29</sup> with 2.25 cm<sup>2</sup>. A fine control over the film formation is required to obtain a homogeneous film surface, and morphological differences may lead to different responses caused by the 16 IR-LEDs. Figure 2 displays a top view (panel a) and a cross-sectional view (panel b) FESEM images for a 6-bilayer PAMAM/SWNT LbL film. The film exhibits a random and homogeneous distribution of interconnected SWNTs into the dendrimer layers over the entire sensor surface. The angled cross-section view of Figure 2b shows clearly the internal film structure, demonstrating the large interpenetration of SWNTs into the polymeric layers. In addition, the film is highly porous with a large surface area. The interpenetrated, porous structure is desired, as it can act as fast ionic conducting channels. This can be advantageous for (bio)chemical sensors in the FEDs platform, leading to enhanced sensing properties, including a fast response time, stable signal, and high sensitivity. The LbL film adsorbed on the LAPS chips surface was stable against several rinsing processes with aqueous solutions at distinct pH values. The same did not apply to a cast film of raw SWNTs, which exhibited a nonhomogeneous, densely aggregated distribution on the chip surface, in addition to a poor thickness control and poor stability. This contrast confirms the suitability of the LbL technique for processing CNTs in nanostructured films.

The surface morphology of the LbL films was also investigated with AFM images for a scanned area of 2.0 × 2.0 μm<sup>2</sup>, for which the same LAPS samples used in the electrical

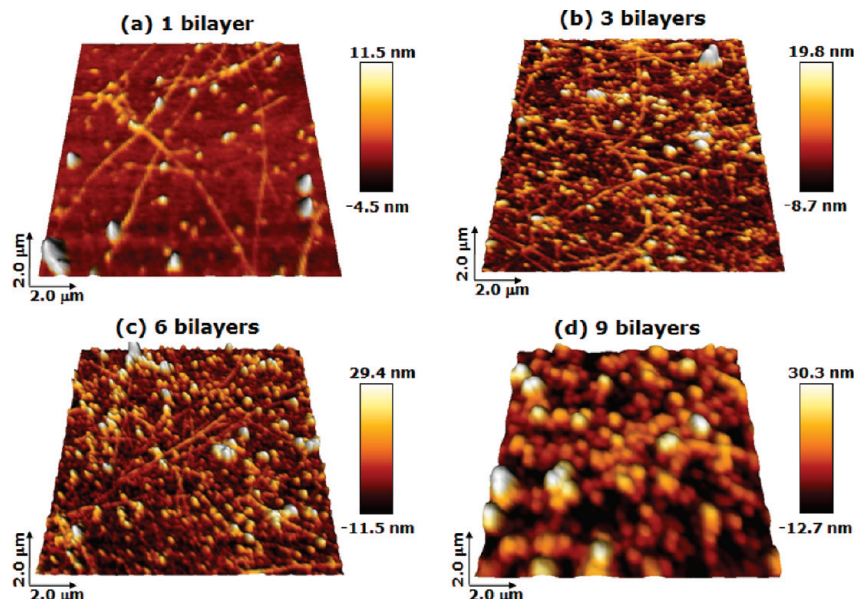


**Figure 3.** AFM images for a PAMAM/SWNT LbL film at different numbers of bilayers.

**TABLE 1: Roughness and Thickness of PAMAM/SWNT LbL Films at Different Bilayers**

no. of bilayers	rms roughness (nm)	thickness (nm)
1	2	8
3	12	40
6	9	43
9	7	47

experiments and to obtain the FESEM images were employed. For a 1-bilayer film, Figure 3a shows that the LAPS chips surface was not fully covered, displaying a random, interconnected network of bundled SWNTs with an average diameter of 3–5 nm. After deposition of 3 bilayers, the sensor surface was entirely covered by a dense, highly porous nanofilm, as shown in Figure 3b that displays interconnection of the SWNTs network into the dendrimer layers. A similar morphology was observed for a 6-bilayer film presented in Figure 3c, now with increasing aggregation of dendrimers. This tendency is confirmed in the 9-bilayer LbL film of Figure 3d, which surface contains a dense packing of dendrimer aggregates. This latter, thicker film presented lesser porosity and roughness, as indicated by the values of the root-mean-square (rms) roughness in Table 1. The film thickness was also affected by the dendrimer packing, as Table 1 indicates only a very small increase in thickness for films with more than 3 bilayers. This finding may be related to the saturation in the potential shifts after adsorption of the eighth bilayer depicted in Figure 1c. The formation of a uniform, densely packed structure may hinder the detection of the potential difference across the solid/liquid interface, which is consistent with the loss in sensitivity reported for thicker LbL films applied in sensing.<sup>22,25</sup>

**3.3. pH Sensitivity and Penicillin Sensing Ability of the Modified LAPS.** Figure 4 shows the investigation of the pH sensitivity of the modified LAPS with PAMAM/SWNT LbL films (LAPS-NT), using commercial buffered solutions. The sensor chip was submitted to different buffered solutions from 3 to 10 and the measurements started after stabilization of the signal. The electrochemical characterization of the pH sensitivity is necessary since the operation principle of a field-effect (bio)chemical sensor (EIS or LAPS) is based on detection of  $H^+$  ions at the transducer/analyte interface; this is especially important when detecting hydrolase-based enzymatic reaction

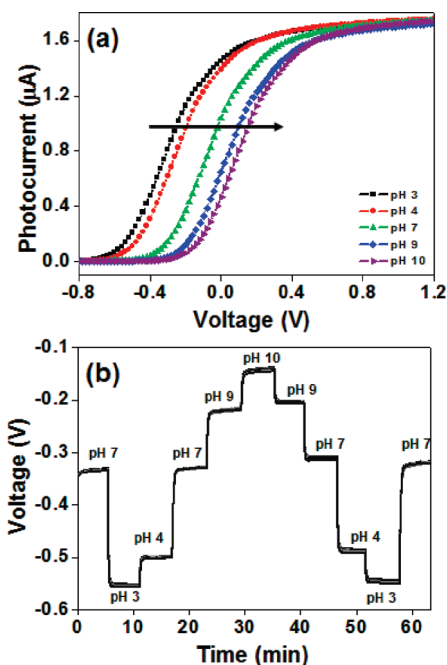
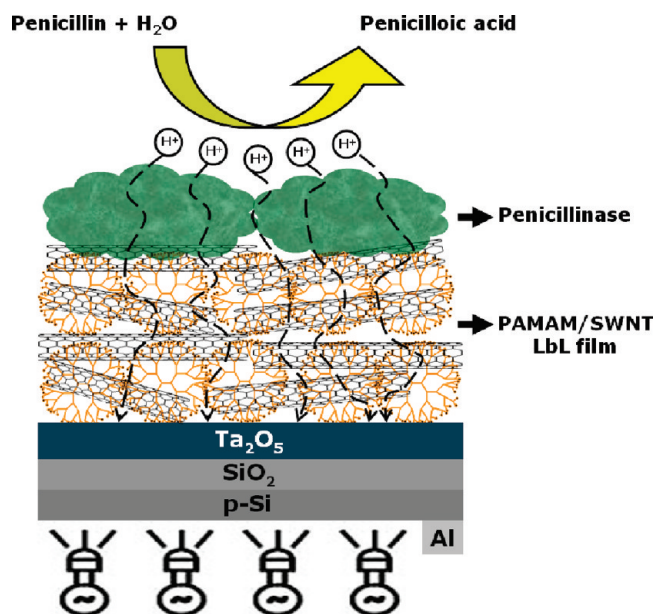


**Figure 4.** *I/V* curves (a) and CC response (b) at different pH values for the 16 spots of the LAPS-NT sensor.

between an immobilized enzyme (e.g., penicillinase, glucose oxidase) on the sensor with an analyte (e.g., penicillin, glucose) in solution.<sup>3,4,29,30</sup> Panels a and b of Figure 4 show *I/V* curves and CC responses for pH values ranging from 3 to 10, respectively. The CC measurements were reproducible for all 16 spots, revealing that the LAPS-NT sensor exhibits good stability, small drift, fast response time, and low hysteresis (ca. 5 mV). Taking as reference the pH sensitivity of a measured LAPS structure with  $Ta_2O_5$  (ca. 58 mV/pH) without NTs, the presence of the LbL film, containing up to 6 bilayers, did not cause changes in the pH sensitivity of the LAPS structure. However, a small decrease in the pH sensitivity occurred for the 9-bilayer film (ca. 55 mV/pH), which may be correlated with the film morphology observed in the AFM images (see Figure 3d). One should note that a small film thickness and high porosity are important for channels to be established for



**SCHEME 2: Idealized Representation of the Chemical Reaction for a Penicillin Biosensor-Based LAPS Structure Functionalized with PAMAM/SWNT LbL Film Containing Penicillinase**



$H^+$  ions to cross the film and to reach the  $Ta_2O_5$  surface immediately. In this context, the slightly decreased pH sensitivity, observed for LAPS-NT with 9 bilayers or more, is consistent with the close packing of dendrimers discussed in the last subsection. It is stressed that the pH sensitivity experiments were carried out with the same LAPS chip used to perform the electrical experiments depicted in Figure 1.

To investigate the biosensing ability of the LAPS-NT, a new set of nominally identical sensors were carefully prepared and the enzyme penicillinase (PEN) was immobilized on the PAMAM/SWNT films and measurements for penicillin G detection were performed. The choice of penicillin G was motivated by its importance in food control, as its residues (e.g., in milk) can be harmful for human beings.<sup>29,30</sup> This biosensor detects changes in the  $H^+$  ion concentration owing to the catalyzed hydrolysis of penicillin into penicilloic acid by the enzyme penicillinase,<sup>4,28,29</sup> as illustrated in Scheme 2. Figure 5a shows a dynamic CC response for a bare LAPS and a 3-bilayer LAPS-NT sensor toward penicillin G detection at concentrations from  $0.5 \times 10^{-3}$  to  $5.0 \times 10^{-3}$  mol  $L^{-1}$ , where the measurement for each solution was alternated with buffer solution measurements. The concentration range was chosen based on reported field-effect penicillin biosensors.<sup>4,29,30</sup> The LAPS-NT penicillin biosensor was found to be reproducible in this series of nominally identical sensing units, being highly sensitive for penicillin G with ca. 100 mV/decade to be compared with ca. 79 mV/decade for the bare LAPS. This was confirmed in the calibration curves in Figure 5b. The higher sensitivity of the modified LAPS may also be attributed to the nanoporous morphology of the LbL films depicted in Figures 2 and 3, which improved penetration of  $H^+$  ions through the film. Furthermore, the large surface areas inherent in the LbL films may lead to the stable adsorption of a number of different enzymes.

Because the LbL films were produced from charged materials whose properties depend on the pH, one could argue that an intrinsic pH dependence could mask the results in the sensing experiments. However, this should not occur for the following

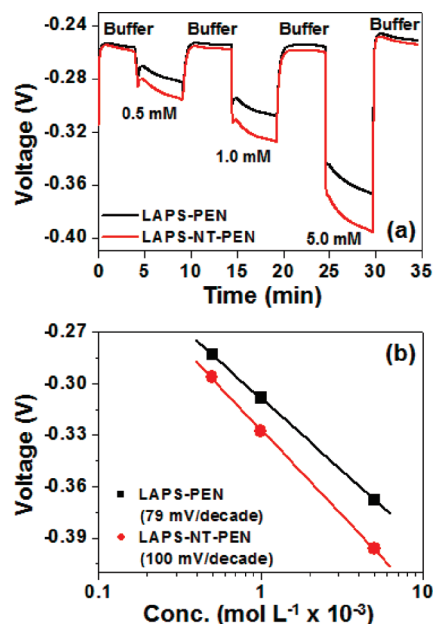


**Figure 5.** CC response at different penicillin concentrations for a bare LAPS and a LAPS-NT sensor (a) and corresponding calibration curves and sensitivity (b).

reasons. Both PAMAM and functionalized CNTs can be considered “weak” electrolytes with the ionization degree varying with pH, which then affects the adsorption of the LbL films. This is why we set the pHs of the dipping solutions at 4 and 8 for PAMAM and CNTs, respectively, ensuring they were both charged to promote an efficient electrostatic interaction for adsorption. After deposition of the PAMAM/SWNTs on the gate of the FETs, however, there should not be many free amino and COOH groups, for they interact within the multilayers. Charges are compensated through electrostatic interactions, which are not supposed to be disrupted in the pH range employed, otherwise the films would dissolve. Then, with such stability the change in pH during the sensing experiments is not expected to affect the film properties and cause artifacts in the measurements.

The results presented here demonstrate that LAPS surfaces covered with LbL films may appear as promising new sensor platforms suitable for the integration of a biological recognition element into a semiconductor field-effect device. Also worth mentioning was the simultaneous monitoring of 16 spots on the same film.

#### 4. Conclusions

To our knowledge, this is the first report of a layer-by-layer assembly of carbon nanotubes on light-addressable potentiometric sensors. With the LAPS platform, the alternated adsorption of PAMAM and SWNT layers could be monitored at each adsorption step. The LbL films displayed a highly porous structure with large surface areas, as indicated by FESEM and AFM images. This structure comprised an interconnection of the SWNTs network into the dendrimers layers, which was essential for the high sensitivity of the biosensors. Indeed, the incorporation of PAMAM/SWNT LbL films onto the LAPS structure led to sensors with high pH sensitivity even in the presence of 6 PAMAM/SWNT bilayers. When a layer of penicillinase was adsorbed on the LbL film, the resulting LAPS-NT-penicillinase structure was highly sensitive to penicillin G, with ca. 100 mV/decade change observed in CC measurements. The enhanced performance is assigned to the morphological

changes induced by CNTs on the sensing units. As for their interesting electrical properties, widely mentioned in the literature, our data are not sufficient to conclude whether the electrical properties had any role in enhancing the sensing performance.

The concept of a controlled film architecture adsorbed on LAPS surfaces, as described here, opens the way for enhanced (bio)chemical sensors containing carbon nanotubes integrated into field-effect devices. This new strategy appears as a possible way to bridge the world of versatile materials for sensing with the well-established silicon device technology.

**Acknowledgment.** The authors thank H.-P. Bochem for the FESEM images. Financial support from CAPES (Brazil) is gratefully acknowledged.

## References and Notes

- (1) Poghosian, A.; Schöning, M. J. Silicon-based chemical and biological field-effect sensors. In *Encyclopedia of Sensors*; Grimes C. A., Dickey E. C., Pishko M. V., Eds.; American Scientific Publishers: Stevenson Ranch, CA, 2006; Vol. 9, p 463.
- (2) Schöning, M. J.; Poghosian, A. Detection of charged macromolecules by means of field-effect devices (FEDs): possibilities and limitations. In *Electrochemical Sensors, Biosensors and Their Biomedical Applications*; Zhang, X., Ju, H., Wang, J., Eds.; Elsevier: Amsterdam, The Netherlands, 2008; Chapter 7, p 187.
- (3) Schöning, M. J.; Poghosian, A. *Electroanalysis* **2006**, *18*, 1893.
- (4) Poghosian, A.; Schöning, M. J.; Schroth, P.; Simonis, A.; Lüth, H. *Sens. Actuators, B* **2001**, *76*, 519.
- (5) Mourzina, Y. G.; Ermolenko, Y. E.; Yoshinobu, T.; Vlasov, Y.; Iwasaki, H.; Schöning, M. J. *Sens. Actuators, B* **2003**, *91*, 32.
- (6) Yoshinobu, T.; Iwasaki, H.; Ui, Y.; Furuichi, K.; Ermolenko, Y.; Mourzina, Y.; Wagner, T.; Näther, N.; Schöning, M. J. *Methods* **2005**, *37*, 94.
- (7) Wagner, T.; Schöning, M. J., Light-addressable potentiometric sensors (LAPS): recent trends and applications. In *Electrochemical Sensor Analysis*; Alegret, S., Merkoci, A., Eds.; Elsevier: Amsterdam, The Netherlands, 2007; Vol. 49, p 87.
- (8) Wagner, T.; Rao, C.; Kloock, J. P.; Yoshinobu, T.; Otto, R.; Keusgen, M.; Schöning, M. J. *Sens. Actuators, B* **2006**, *118*, 33.
- (9) Wagner, T.; Molina, R.; Yoshinobu, T.; Kloock, J. P.; Biselli, M.; Canzoneri, M.; Schnitzler, T.; Schöning, M. J. *Electrochim. Acta* **2006**, *53*, 305.
- (10) Balasubramanian, K.; Burghard, M. *Anal. Bioanal. Chem.* **2006**, *385*, 452.
- (11) Kim, S. N.; Rusling, J. F.; Papadimitrakopoulos, F. *Adv. Mater.* **2007**, *19*, 3214.
- (12) Allen, B. L.; Kichambare, P. D.; Star, A. *Adv. Mater.* **2007**, *19*, 1439.
- (13) Javey, A. *ACS Nano* **2008**, *2*, 1329.
- (14) Byon, H. R.; Choi, H. C. *J. Am. Chem. Soc.* **2006**, *128*, 2188.
- (15) Star, A.; Gabriel, J.-C. P.; Bradley, K.; Grüner, G. *Nano Lett.* **2003**, *3*, 459.
- (16) Grüner, G. *Anal. Bioanal. Chem.* **2006**, *384*, 322.
- (17) Oliveira, O. N., Jr.; Zucolotto, V.; Balasubramanian, S.; Li, L.; Nalwa, H. S.; Kumar, J.; Tripathy, S. K. Layer-by-layer polyelectrolyte-based thin films for electronic and photonic applications. In *Handbook of Polyelectrolytes and Their Applications*; Tripathy, S. K., Kumar, J., Nalwa, H. S., Eds.; American Scientific Publishers: Los Angeles, CA, 2002; Vol. 1, p 1.
- (18) Lutkenhaus, J. L.; Hammond, P. T. *Soft Matter* **2007**, *3*, 804.
- (19) Tang, Z.; Wang, Y.; Podsiadlo, P.; Kotov, N. A. *Adv. Mater.* **2006**, *18*, 3203.
- (20) Zucolotto, V.; Daghasanli, K. R. P.; Hayasaka, C. O.; Riul, A.; Ciancaglini, P.; Oliveira, O. N., Jr. *Anal. Chem.* **2007**, *79*, 2163.
- (21) Siqueira, J. R., Jr.; Gasparotto, L. H. S.; Crespiho, F. N.; Carvalho, A. J. F.; Zucolotto, V.; Oliveira, O. N., Jr. *J. Phys. Chem. B* **2006**, *110*, 22690.
- (22) Siqueira, J. R., Jr.; Crespiho, F. N.; Zucolotto, V.; Oliveira, O. N., Jr. *Electrochem. Commun.* **2007**, *9*, 2676.
- (23) Yan, Y.; Zhang, M.; Gong, K.; Su, L.; Guo, Z.; Mao, L. *Chem. Mater.* **2005**, *17*, 3457.
- (24) Yang, M.; Yang, Y.; Yang, H.; Shen, G.; Yu, R. *Biomaterials* **2006**, *27*, 246.
- (25) Siqueira, J. R., Jr.; Gasparotto, L. H. S.; Oliveira, O. N., Jr.; Zucolotto, V. *J. Phys. Chem. C* **2008**, *112*, 9050.
- (26) Lee, S. W.; Kim, B.-S.; Chen, S.; Shao-Horn, Y.; Hammond, P. T. *J. Am. Chem. Soc.* **2009**, *131*, 671.
- (27) Poghosian, A.; Abouzar, M. H.; Amberger, F.; Mayer, D.; Han, Y.; Ingebrandt, S.; Offenhäusser, A.; Schöning, M. J. *Biosens. Bioelectron.* **2007**, *22*, 2100.
- (28) Poghosian, A.; Ingebrandt, S.; Abouzar, M. H.; Schöning, M. J. *Appl. Phys. A: Mater. Sci. Process.* **2007**, *87*, 517.
- (29) Siqueira, J. R., Jr.; Abouzar, M. H.; Bäcker, M.; Zucolotto, V.; Poghosian, A.; Oliveira, O. N., Jr.; Schöning, M. J. *Phys. Status Solidi A* **2009**, *206*, 462.
- (30) Abouzar, M. H.; Poghosian, A.; Razavi, A.; Besmehn, A.; Bijmens, N.; Williams, O. A.; Haenen, K.; Wagner, P.; Schöning, M. J. *Phys. Status Solidi A* **2008**, *205*, 2141.

JP904777T